Extended OVI halos around star-forming galaxies

Evgenii Vasiliev, Marina Ryabova

Southern Federal University, Rostov-on-Don, Russia

modelling of the ionic composition is always based on equilibrium:
photo or collisional

Determination of physical conditions in clouds observed in absorption and characteristics of external radiation

- ✓ metallicity;
- ✓ temperature;
- ✓ number density;
- ✓ cloud size;
- ✓ a shape of the spectrum;

Summary of HVC Column Density Measurements

Component	H I	C II	C III	C IV	Si II	Si III	Si IV	O VI
HE 0226−4110								
HVC1	16.29 ± 0.05	$13.53^{+0.05}_{-0.07}$	$13.28^{+0.06}_{-0.05}$	<13.35	12.65 ± 0.10	$12.22^{+0.16}_{-0.26}$	<12.57	$13.25^{+0.13}_{-0.12}$
HVC2	16.21 ± 0.10	$13.90^{+0.34}_{-0.09}$	$13.59^{+0.70}_{-0.16}$	$13.36^{+0.15}_{-0.21}$	$12.81^{+0.25}_{-0.08}$	$12.76^{+0.07}_{-0.08}$	<12.52	$13.36^{+0.10}_{-0.11}$
HVC3	16.74 ± 0.20[a]	$13.63^{+0.06}_{-0.07}$	$13.92^{+1.00}_{-0.23}$	$13.20^{+0.14}_{-0.19}$	12.70 ± 0.07	12.67 ± 0.09	<12.36	$13.34^{+0.08}_{-0.09}$
HVC4	16.34 ± 0.10	$13.92^{+0.25}_{-0.05}$	$13.90^{+1.00}_{-0.05}$	$13.31^{+0.17}_{-0.24}$	12.71 ± 0.08	$12.89^{+0.28}_{-0.07}$	12.85 ± 0.15	$13.29^{+0.09}_{-0.11}$
PG 0953+414								
HVC1	16.15 ± 0.15	13.57 ± 0.05	...	<12.97	12.57 ± 0.05	12.55 ± 0.07	$12.39^{+0.14}_{-0.19}$	<13.49
HVC2	16.26 ± 0.15	[illegible]	$13.77^{+0.25}_{-0.04}$	$12.99^{+0.13}_{-0.20}$	<12.45	12.90 ± 0.05	$12.34^{+0.16}_{-0.24}$	13.74 ± 0.08

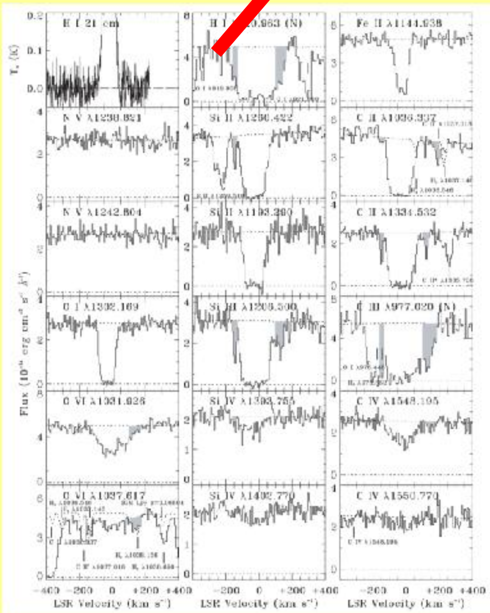

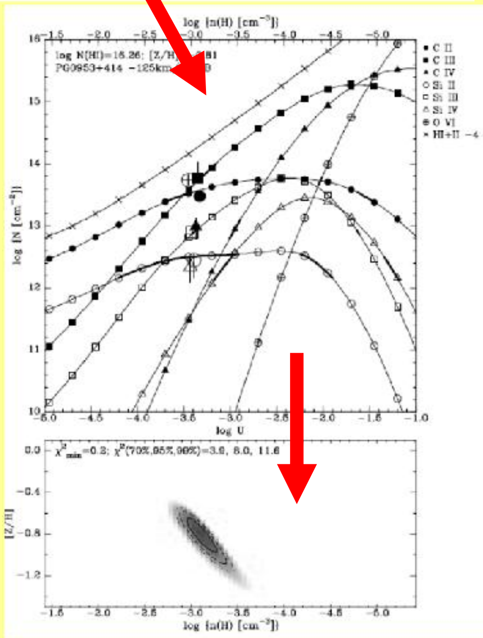

Fox et al 2005

Simcoe et al 2006: simple CLOUDY

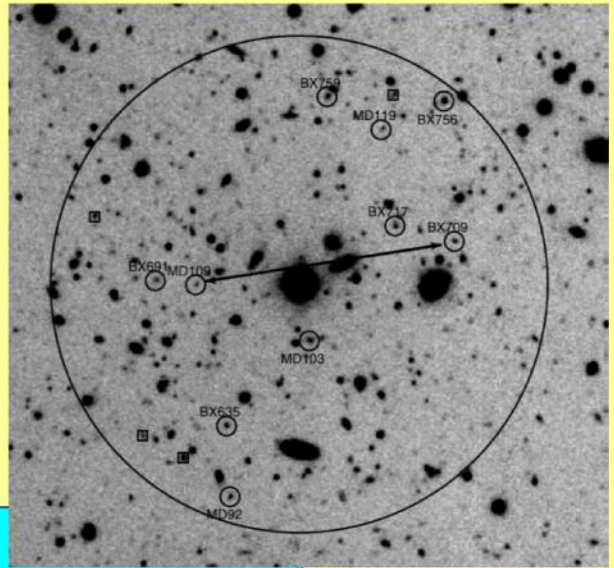

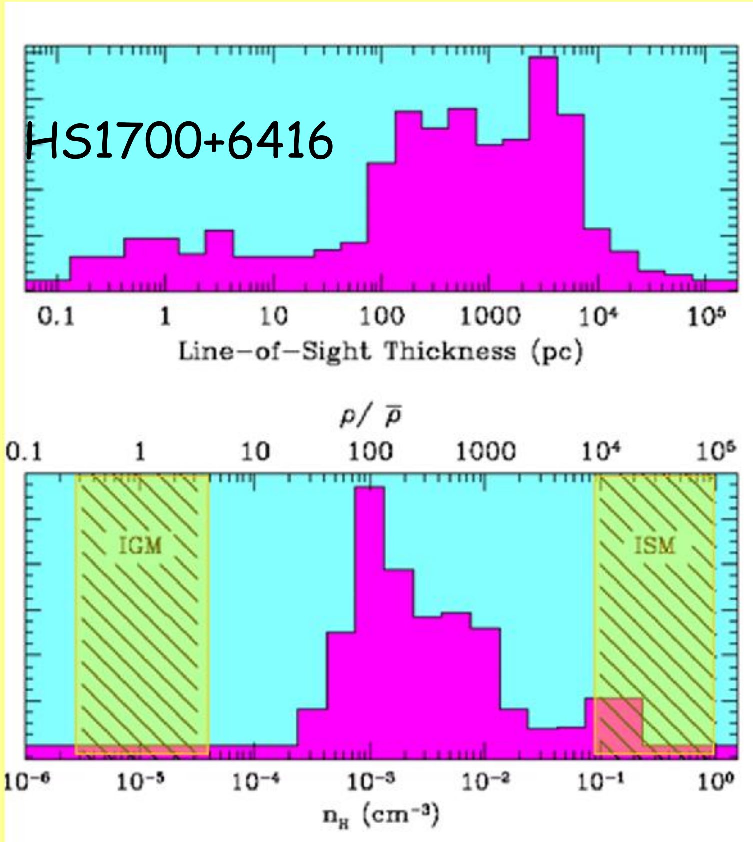

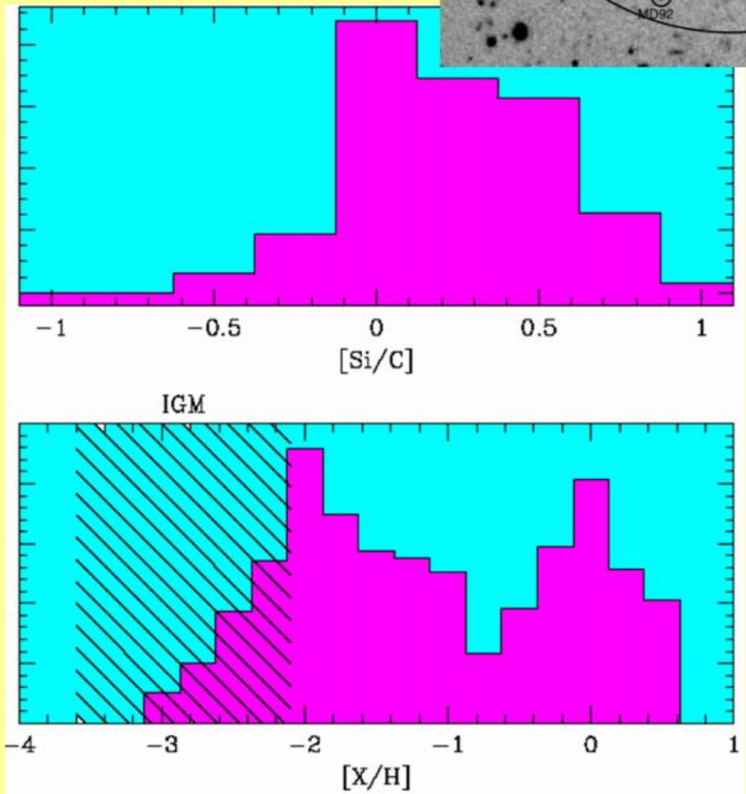

EQ or NEQ?

Equilibrium of Evolution?

dynamical time
(e.g. Hubble, cloud collision …)

cooling time

chemical time
(e.g. recombination time)

density

chemical composition

temperature

UV/Xray spectrum

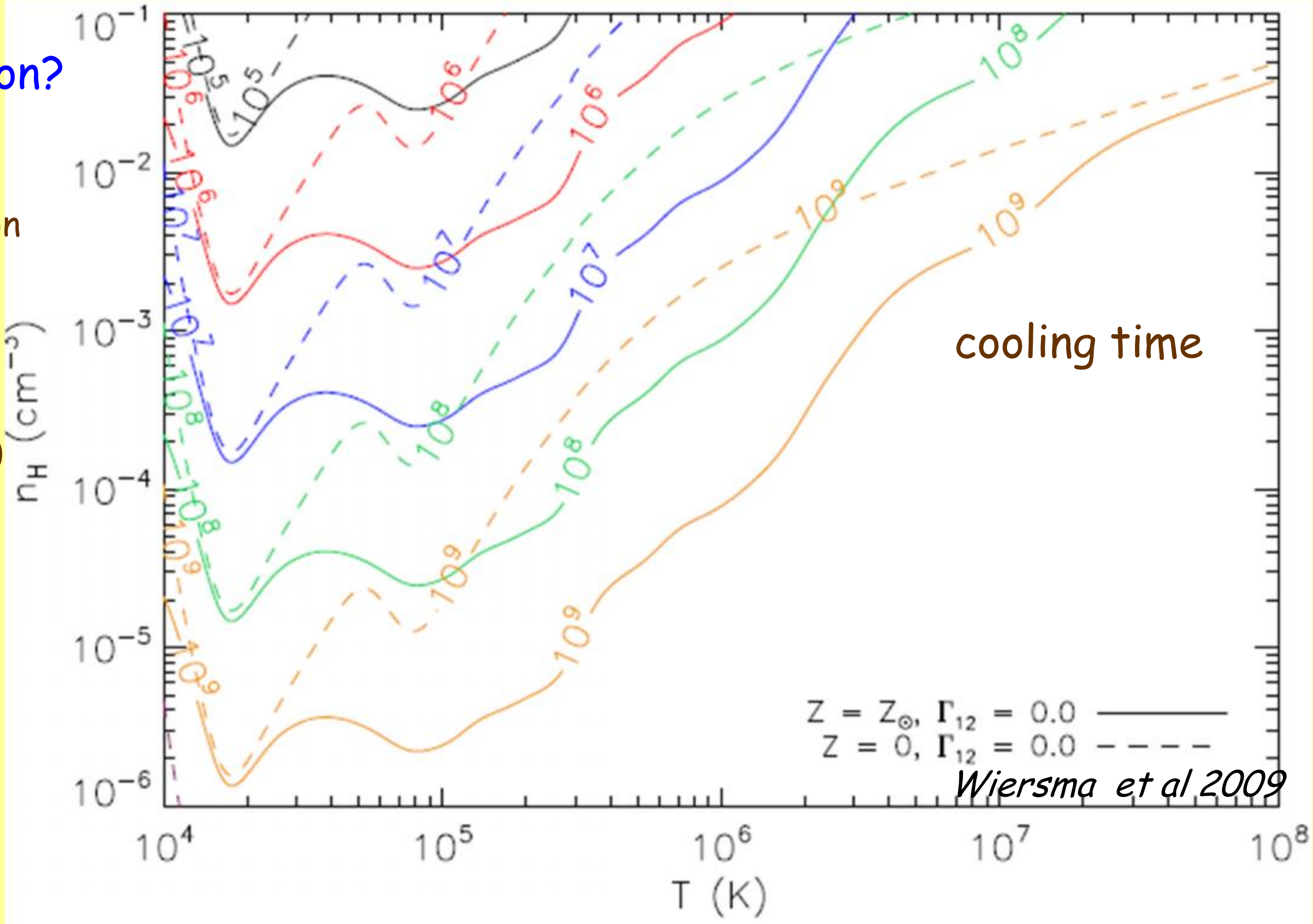

ionic composition of astrophysical plasma: EQ or NEQ

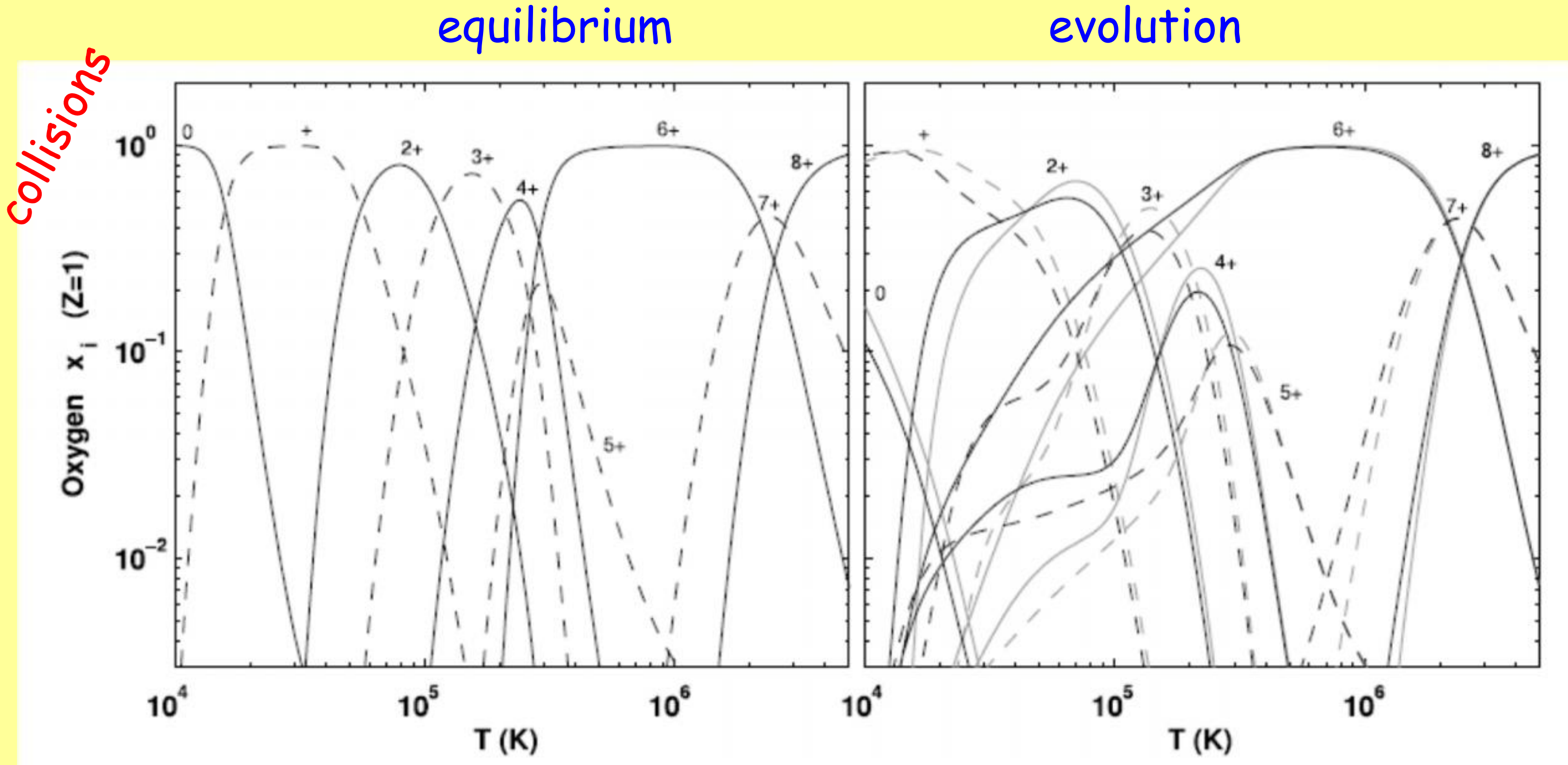

Gnat & Sternberg 2007

more ionized gas in the NEQ

recombination lag

dependence on metallicity

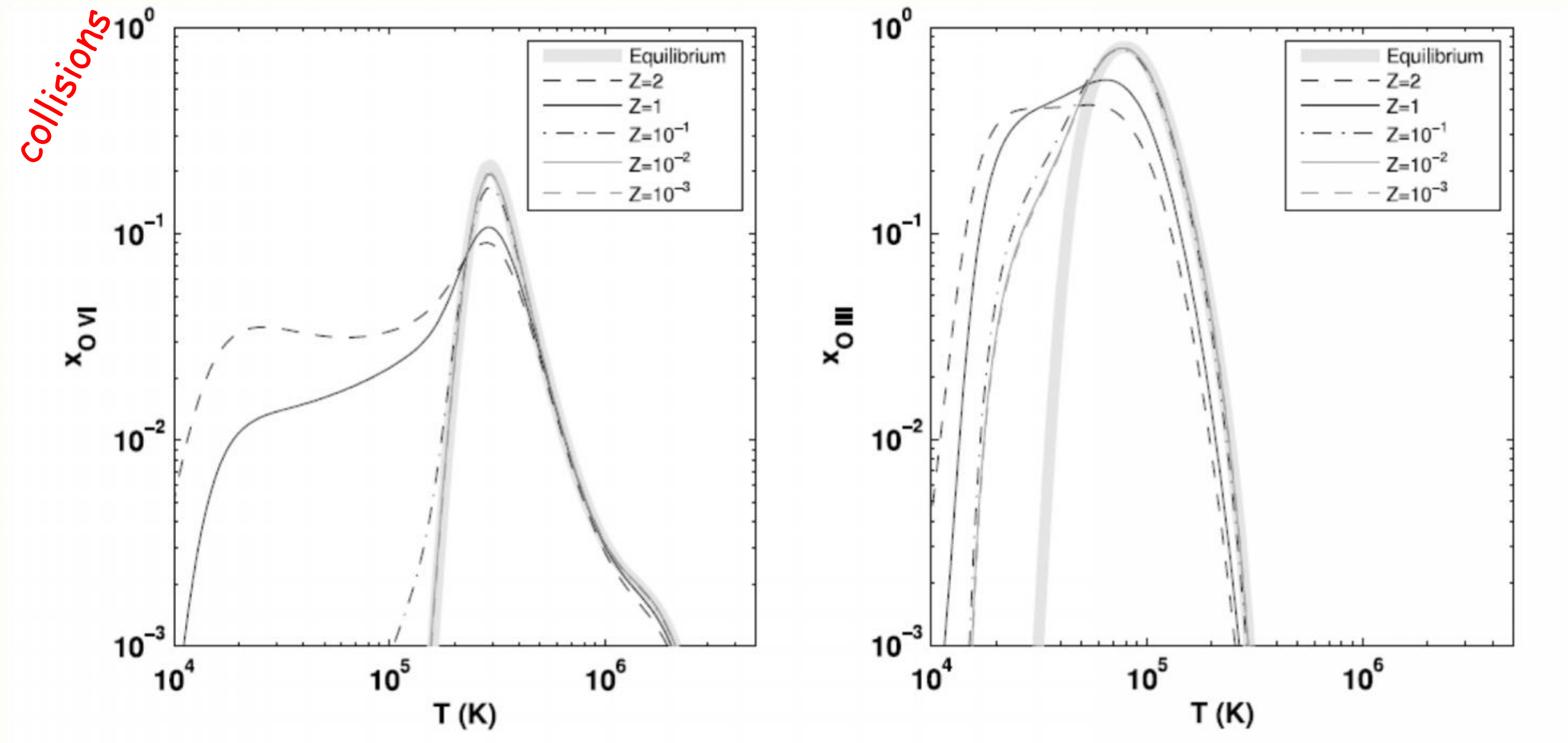

FIG. 3.—O^{5+} (*left*) and O^{++} (*right*) ion fractions vs. temperature for metallicities Z ranging from 10^{-3} to 2, for isochoric cooling. The CIE distributions are shown by the thick gray lines.

Gnat & Sternberg 2007

higher metallicity is faster evolution (more efficient cooling), than NEQ effects (recombination lag) increase

dependence on gas density for photoEQ

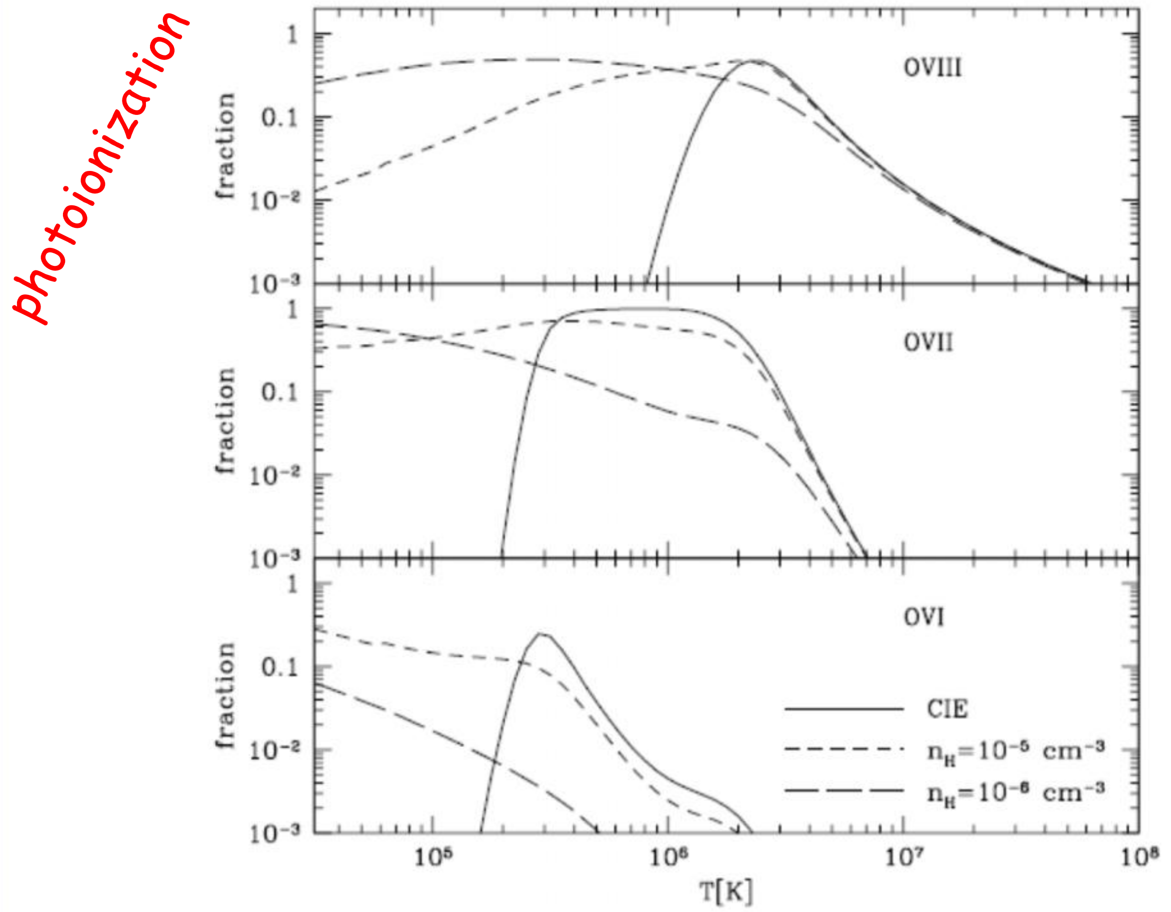

Fig. 2. Ionization fractions of O VI, O VII and O VIII in ionization equilibrium as a function of temperature for the low density plasma with $n_H = 10^{-5}$ and 10^{-6} cm^{-3} under the presence of photoionizing background radiation at a redshift of $z = 0$. Ionization fractions in collisional ionization equilibrium are also shown for the comparison.

Yoshikowa & Sasaki 2004

dependence on gas density for photoNEQ

photoionization

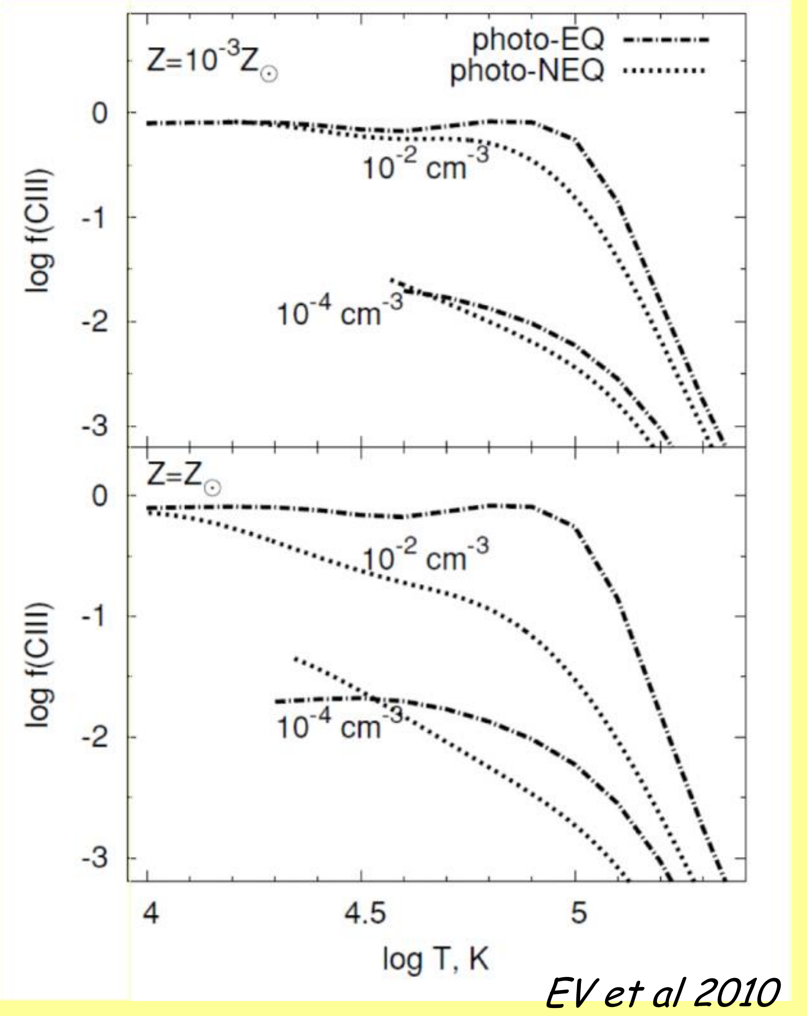

EV et al 2010

metals in the IGM/CGM/ISM: an observational example

not in scale

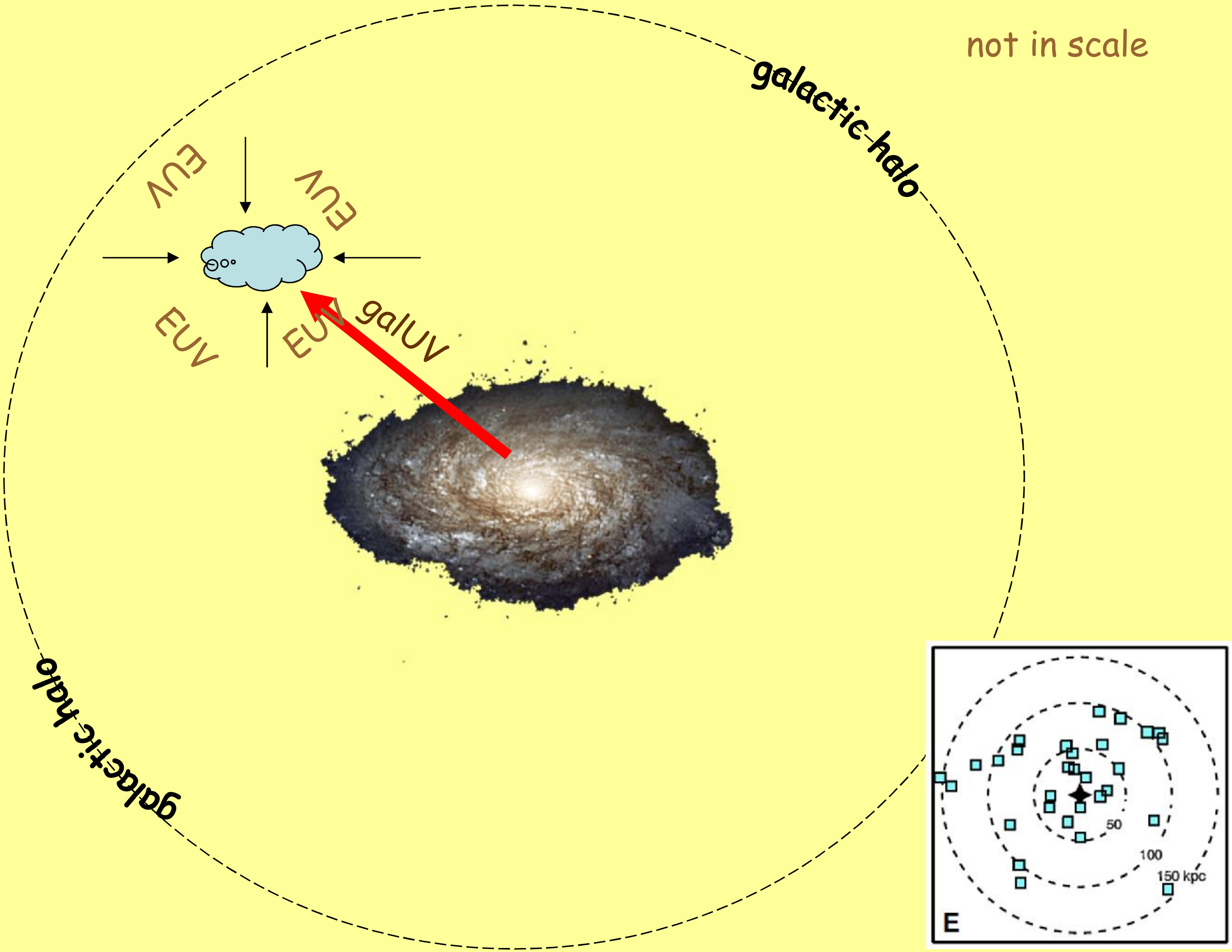

metals in the IGM/CGM/ISM: an example

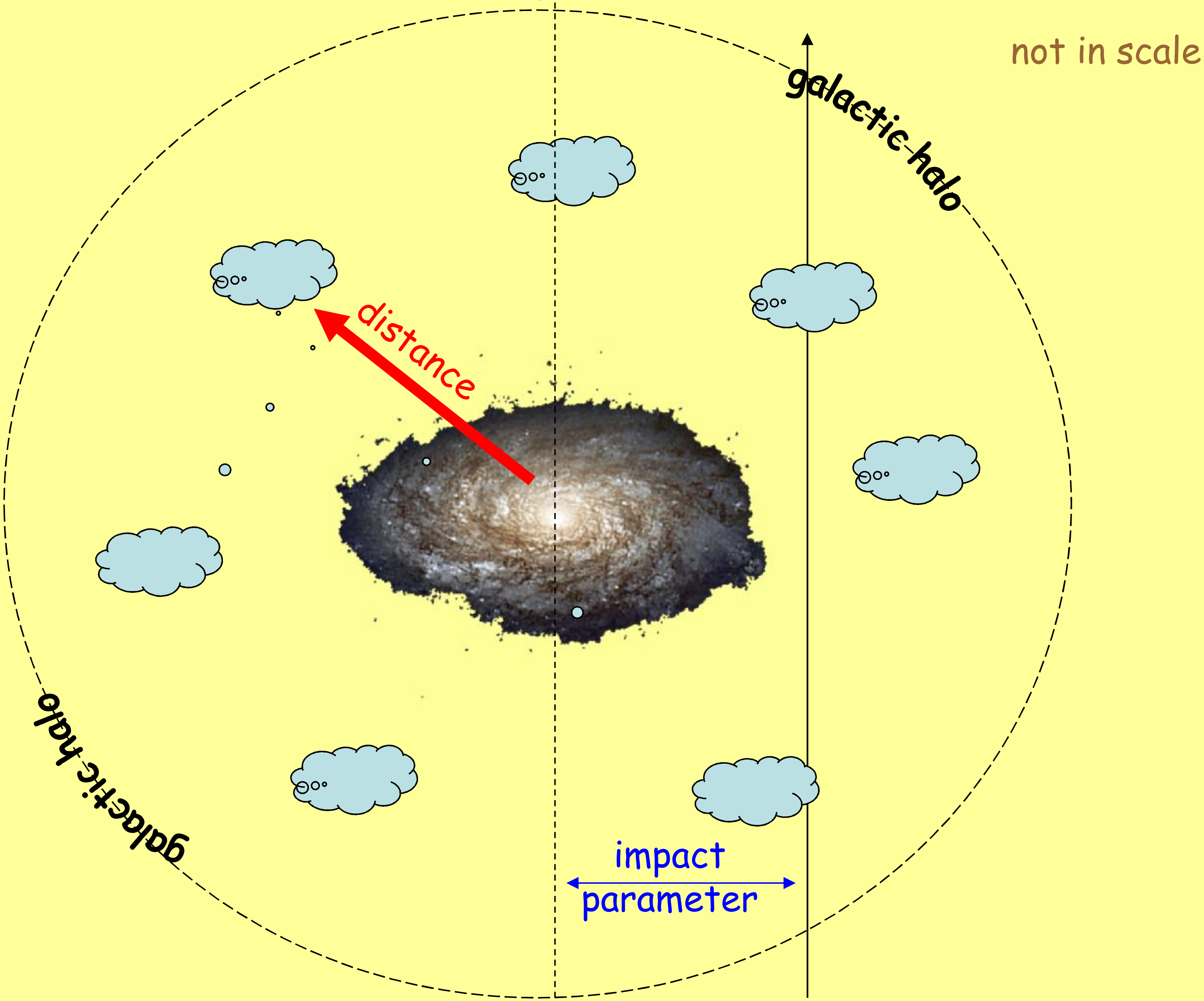

metals in the IGM/CGM/ISM: an observational example: **extremely extended OVI**

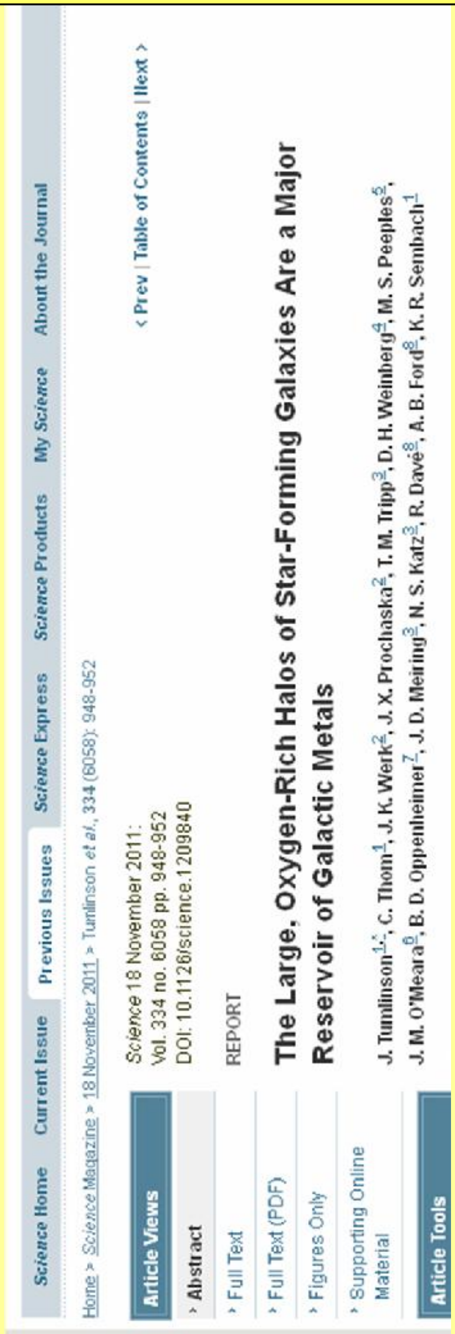

Science Home | Current Issue | Previous Issues | Science Express | Science Products | My Science | About the Journal

Home > Science Magazine > 18 November 2011 > Tumlinson et al., 334 (6058): 948-952

< Prev | Table of Contents | Next >

Article Views
- Abstract
- Full Text
- Full Text (PDF)
- Figures Only
- Supporting Online Material

Article Tools

Science 18 November 2011:
Vol. 334 no. 6058 pp. 948-952
DOI: 10.1126/science.1209840

REPORT

The Large, Oxygen-Rich Halos of Star-Forming Galaxies Are a Major Reservoir of Galactic Metals

J. Tumlinson[1,*], C. Thom[1], J. K. Werk[2], J. X. Prochaska[2], T. M. Tripp[3], D. H. Weinberg[4], M. S. Peeples[5], J. M. O'Meara[6], B. D. Oppenheimer[7], J. D. Meiring[3], N. S. Katz[3], R. Davé[8], A. B. Ford[8], K. R. Sembach[1]

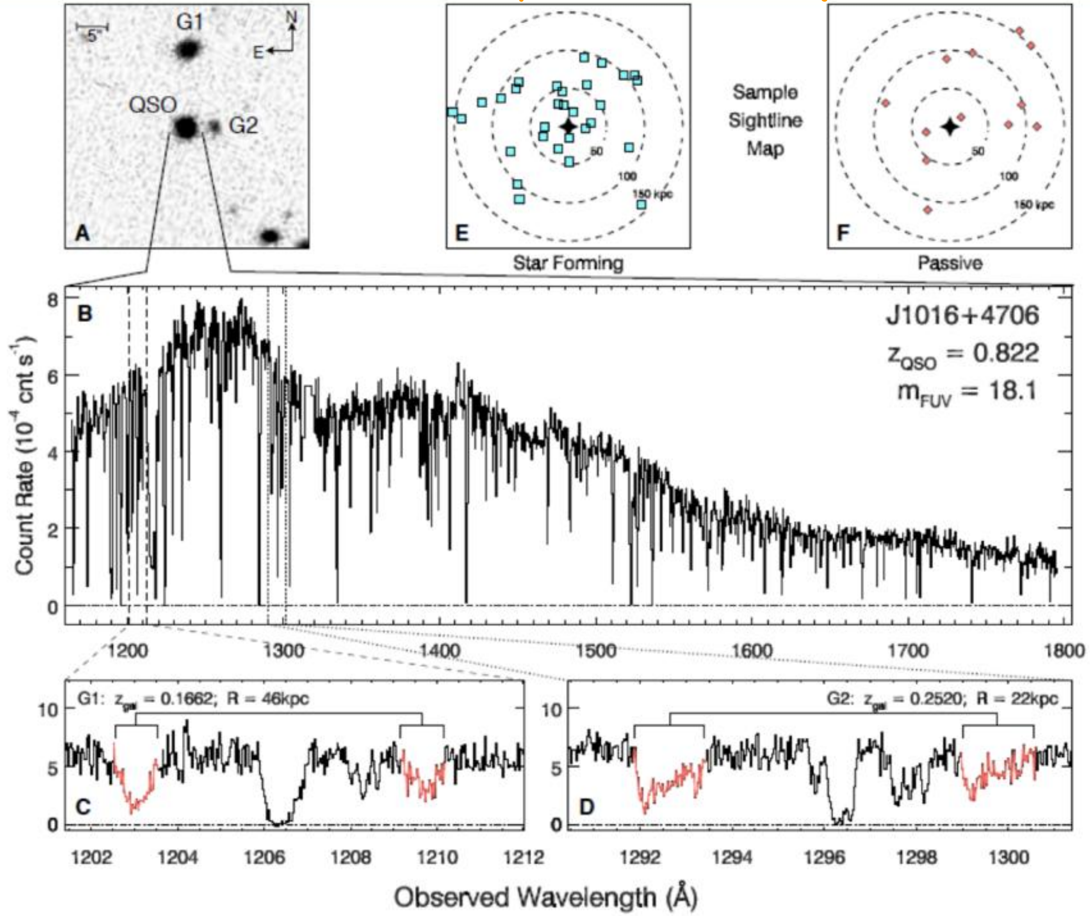

Figure 1: An illustration of our sampling technique and data. (**A**) An SDSS composite image of the field around the QSO J1016+4706 with two targeted galaxies, labeled G1 and G2, which are both in the star-forming subsample. (**B**) The complete COS count-rate spectrum (counts s^{-1}) versus observed wavelength. The panels below concentrate on the redshifted O VI 1032,1038 Å doublet for galaxies G1 (**C**) and G2 (**D**). The upper right panels illustrate the full sample by showing the locations of all sightlines in position angle and impact parameter R with respect to the targeted galaxies, for the star-forming (**E**) and passively evolving (**F**) subsamples. The circles mark $R = 50$, 100, and 150 kpc.

metals in the IGM/CGM/ISM: an observational example: **extremely extended OVI**

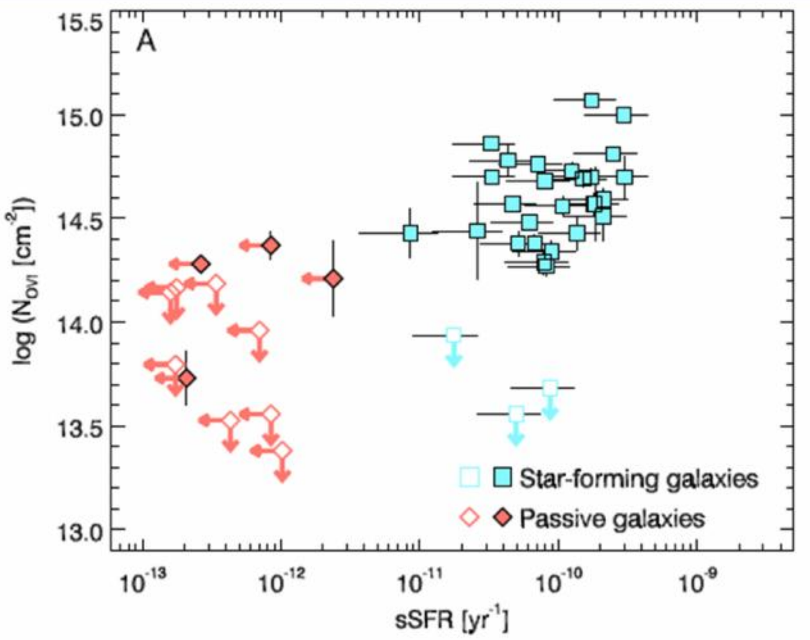

Tumlinson et al 2011

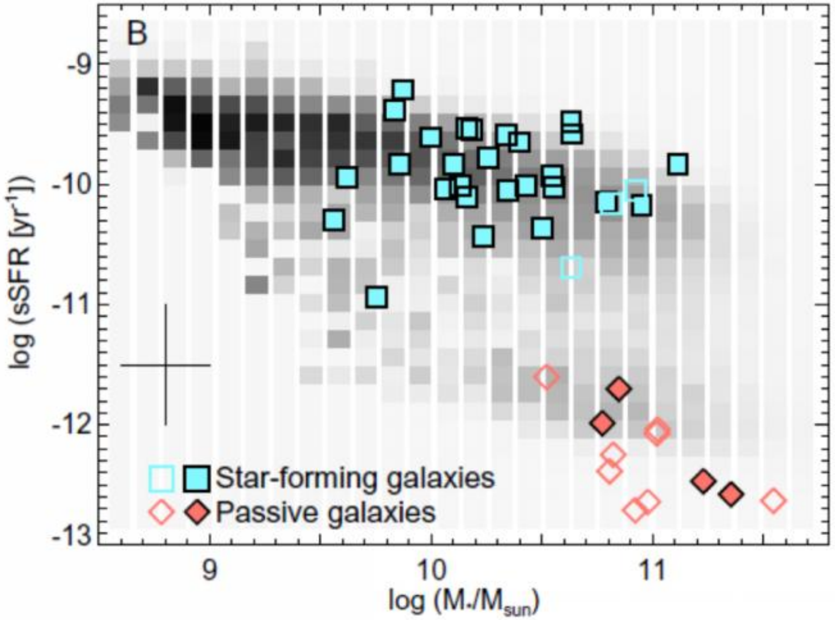

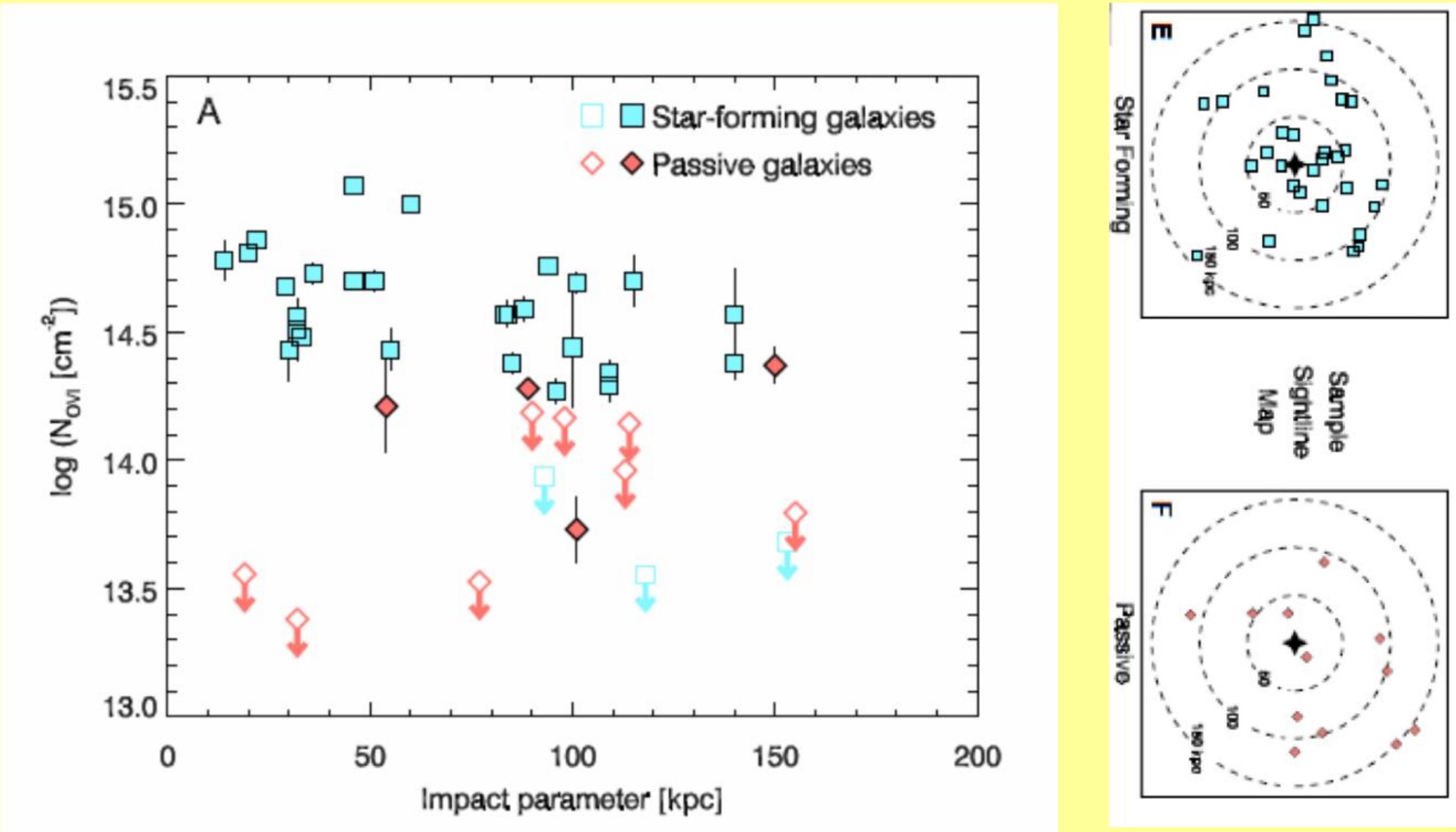

Tumlinson et al 2011

log N(OVI) ~14.2 – 15.1

for star-forming galaxies

too much OVI/oxygen

bounded with the host galaxy

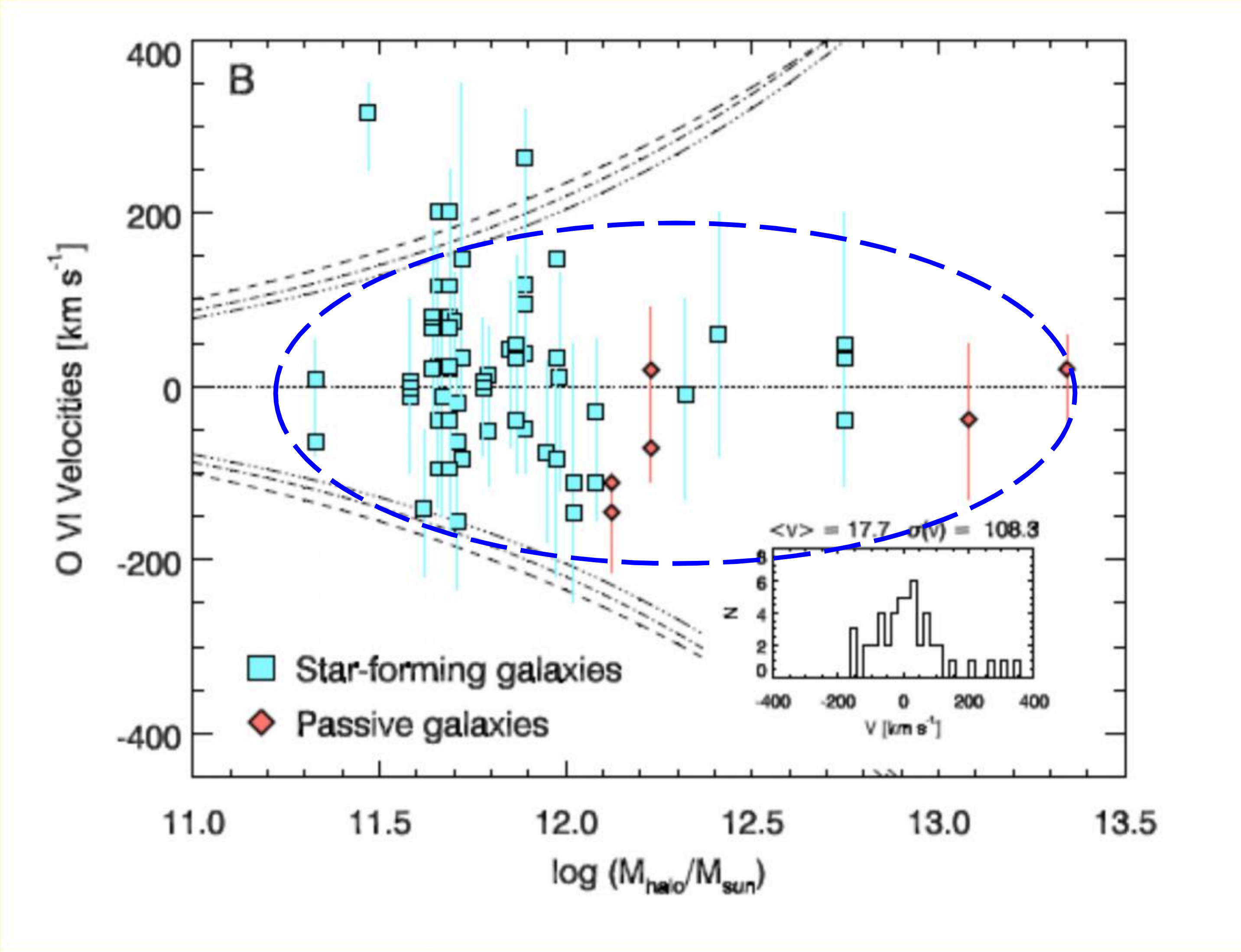

Tumlinson et al 2011

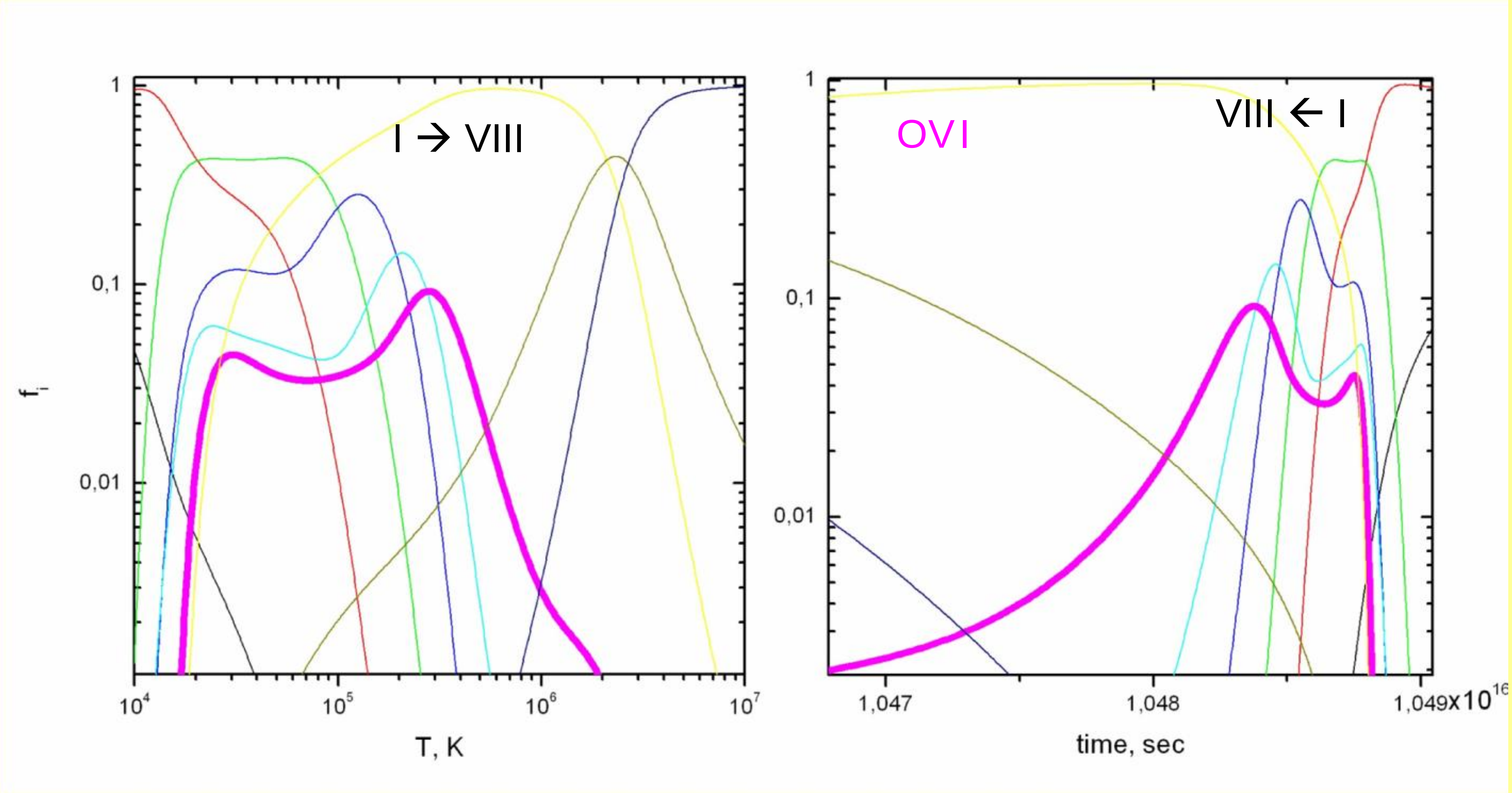

OVI fragility

- the ionization and thermal evolution of gas (in a lagrangian element):
  nonequilibrium (time-dependent) ionization kinetics for H, He, C, N, O, Ne, Mg, Si, Fe and self-consistent cooling and heating rates;

- a power-law SFR: $SFR(t) = M_g^{p_1}/p_2$;

- the galactic halo gas exposed to the cumulative galactic and extragalactic ionizing radiation:

  the extragalactic spectrum: Haardt & Madau (2001) spectra;

  the UV galactic spectrum was calculated using the PEGASE code (Fioc & Rocca-Volmerange 1997);

  the X-ray galactic spectrum calculated using the "LX - SFR'' relation (Gilfanov etal 2004);

  the galactic part of the spectrum being attenuated by the underlying neutral gas with
  $N_{HI} = 10^{20}$ cm^{-2}, $N_{HeI} = 10^{19}$cm^{-2}

not in scale

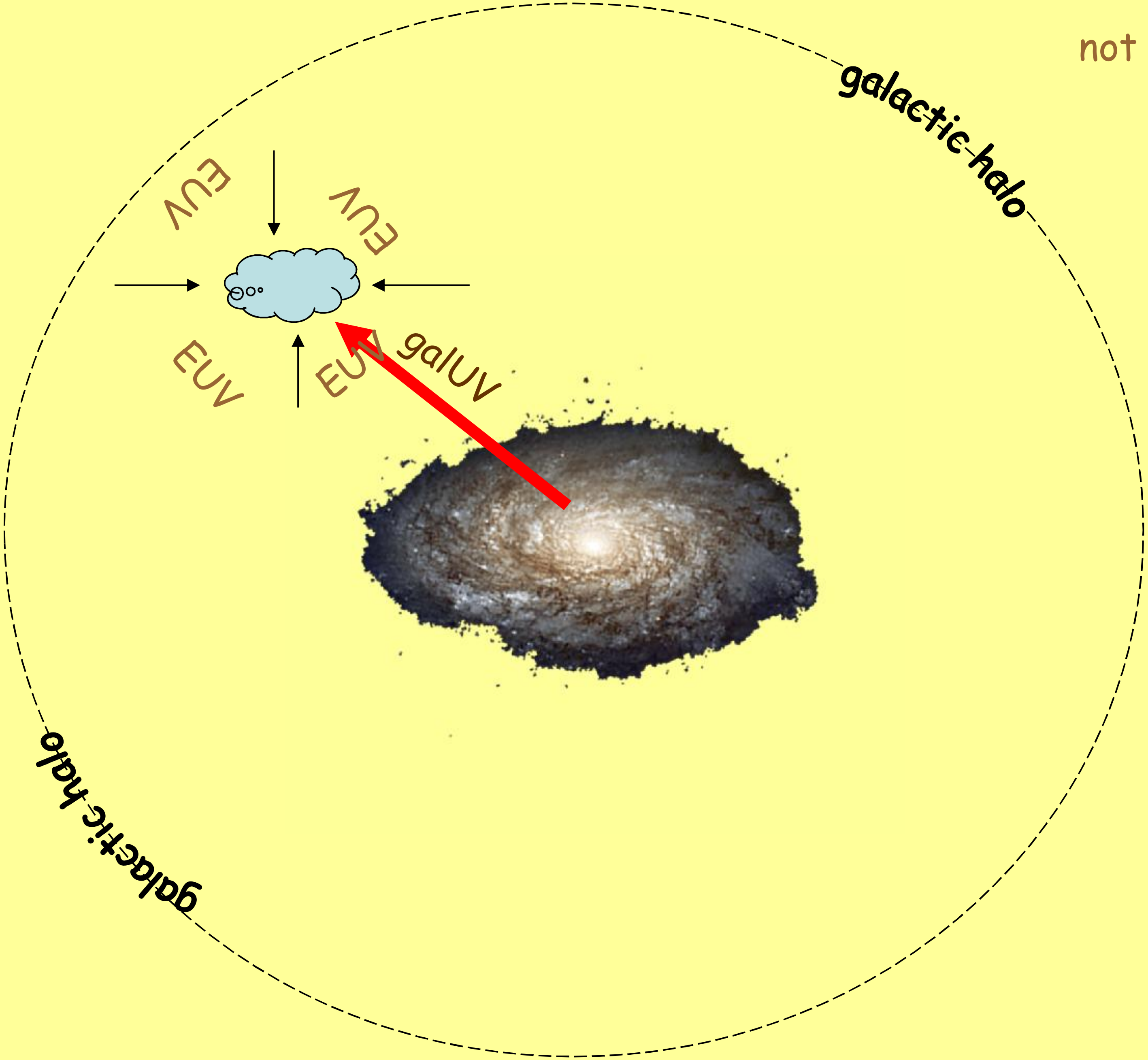

metals in the IGM/CGM/ISM: a model

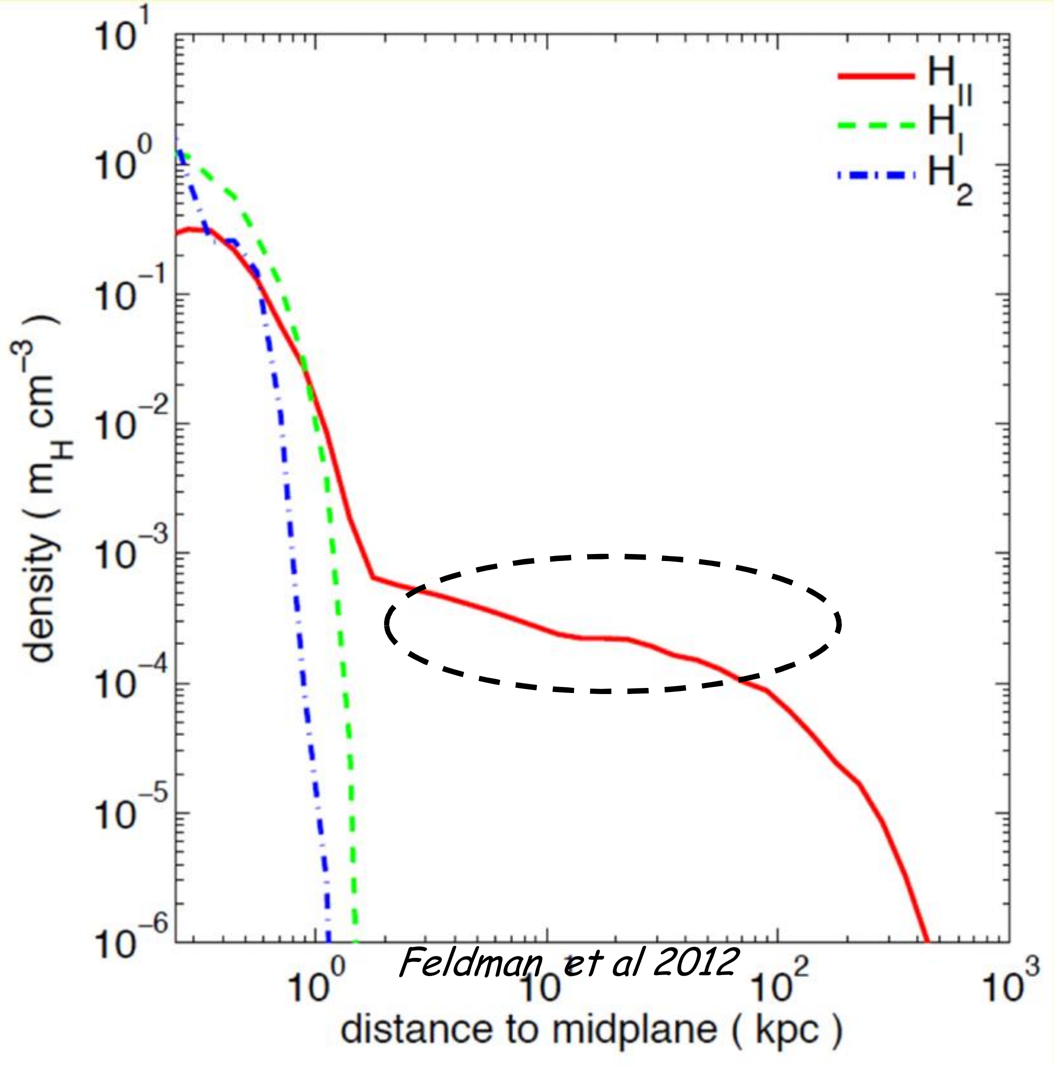

- ✓ the number density ~10^{-4} cm^{-3} at distances ~50-300 kpc (Feldmann etal 2013)
- ✓ we start at z=2 (the lookback time is around 10 Gyrs)
- ✓ the initial gas ionic composition and temperature are set to the ones corresponding to photoequilibrium in gas exposed to the extragalactic Haardt & Madau spectrum at z=2
- ✓ the spectrum is changed in time
- ✓ the gas metallicity ranges from 10^{-2} to 0.1 solar

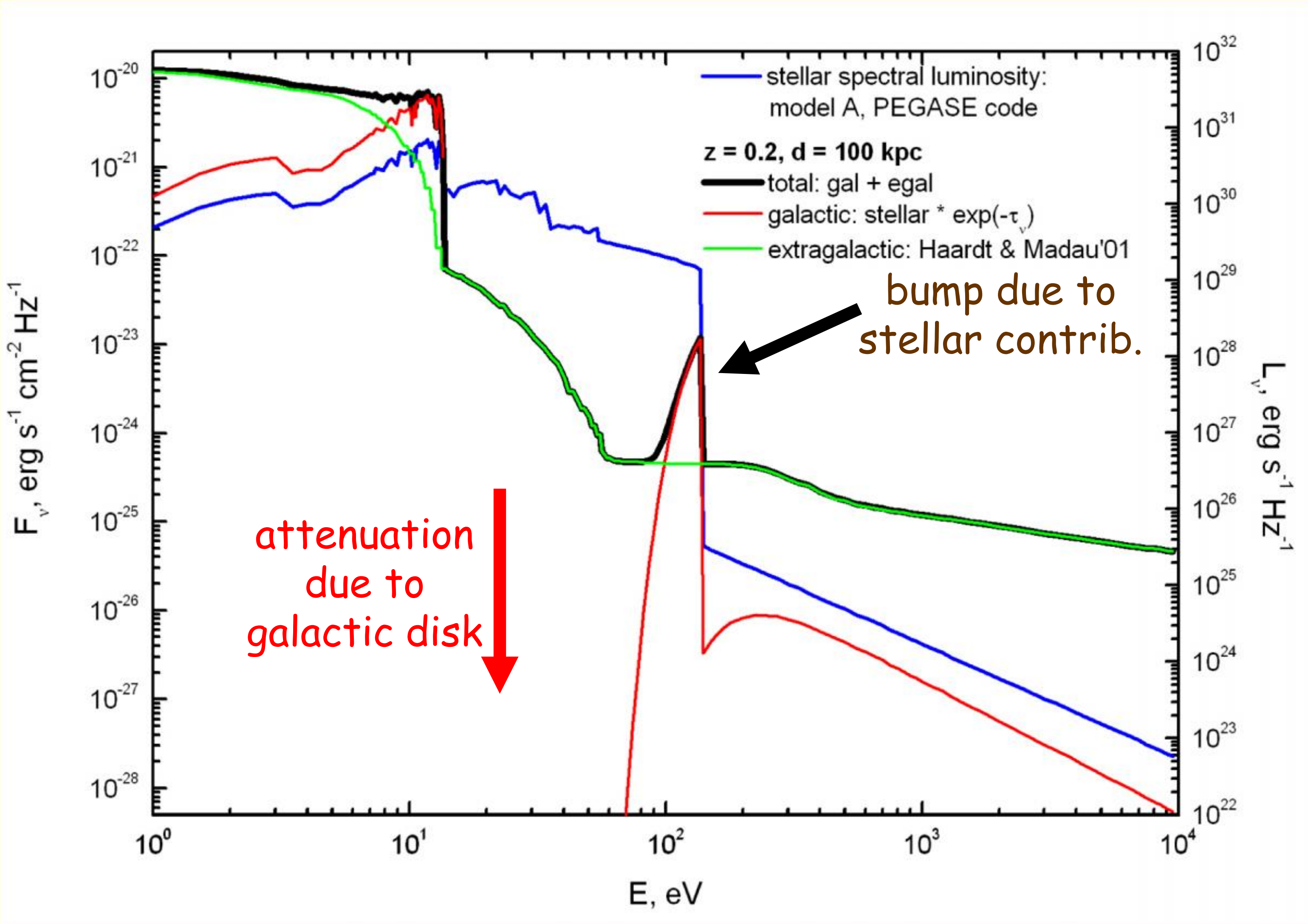

the bump is responsible for OV photoionization

gives higher OVI fraction

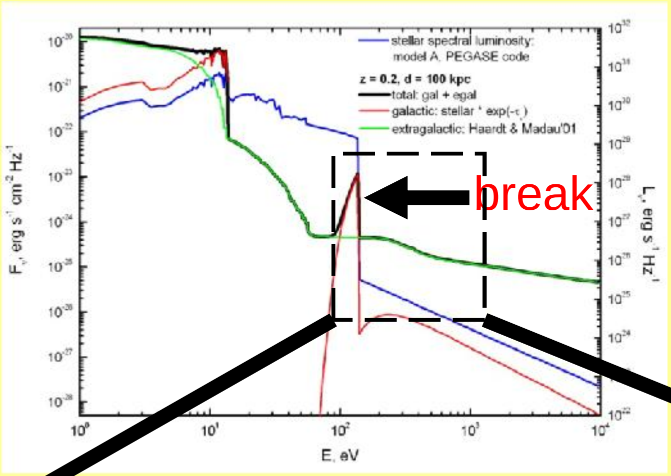

stellar pop codes
(PEGASE and STARBURST99)

give spectra up to **91 Å (136 eV)**

OV -> OVI -> OVII -> OVIII

113.9 138.1 739 eV

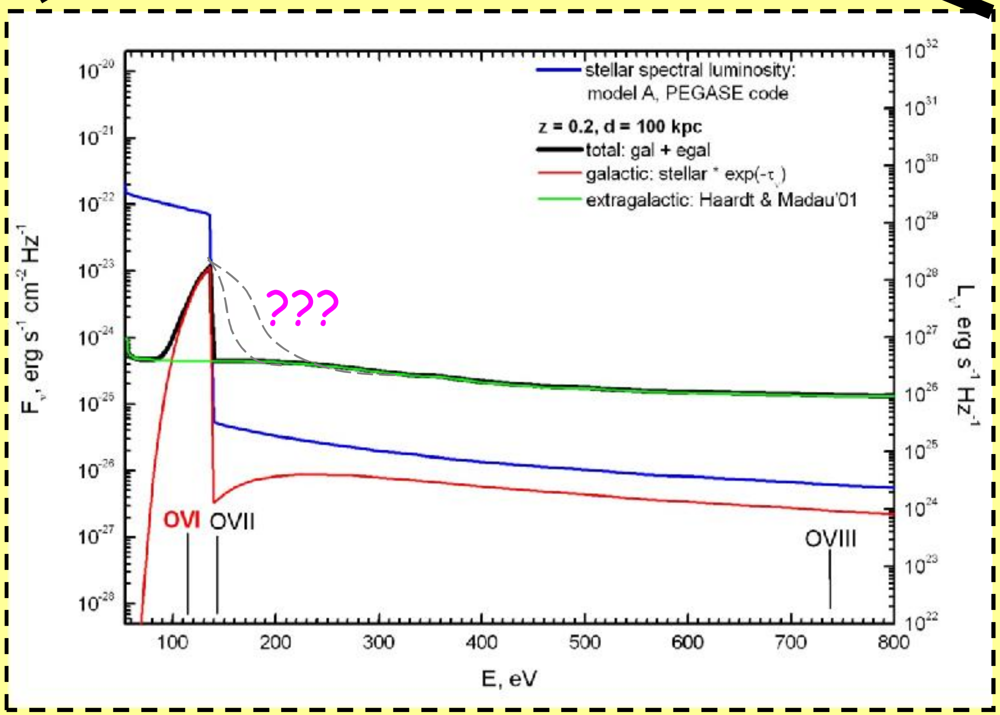

metals in the IGM/CGM/ISM: **implications: circumgalactic OVI**

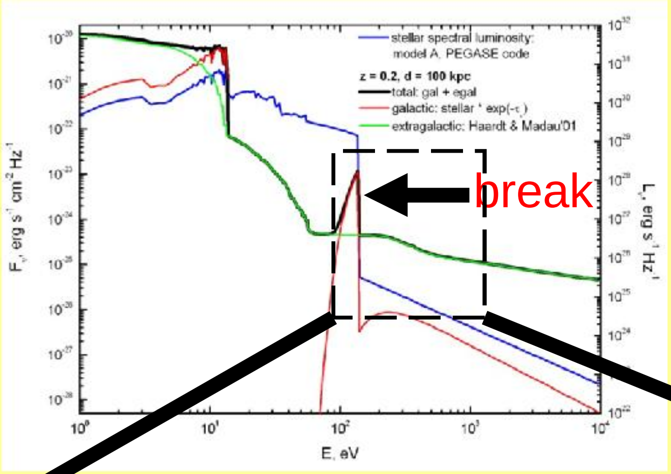

stellar pop codes
(PEGASE and STARBURST99)

give spectra up to **91 Å (136 eV)**

OV -> OVI -> OVII -> OVIII

113.9 138.1 739 eV

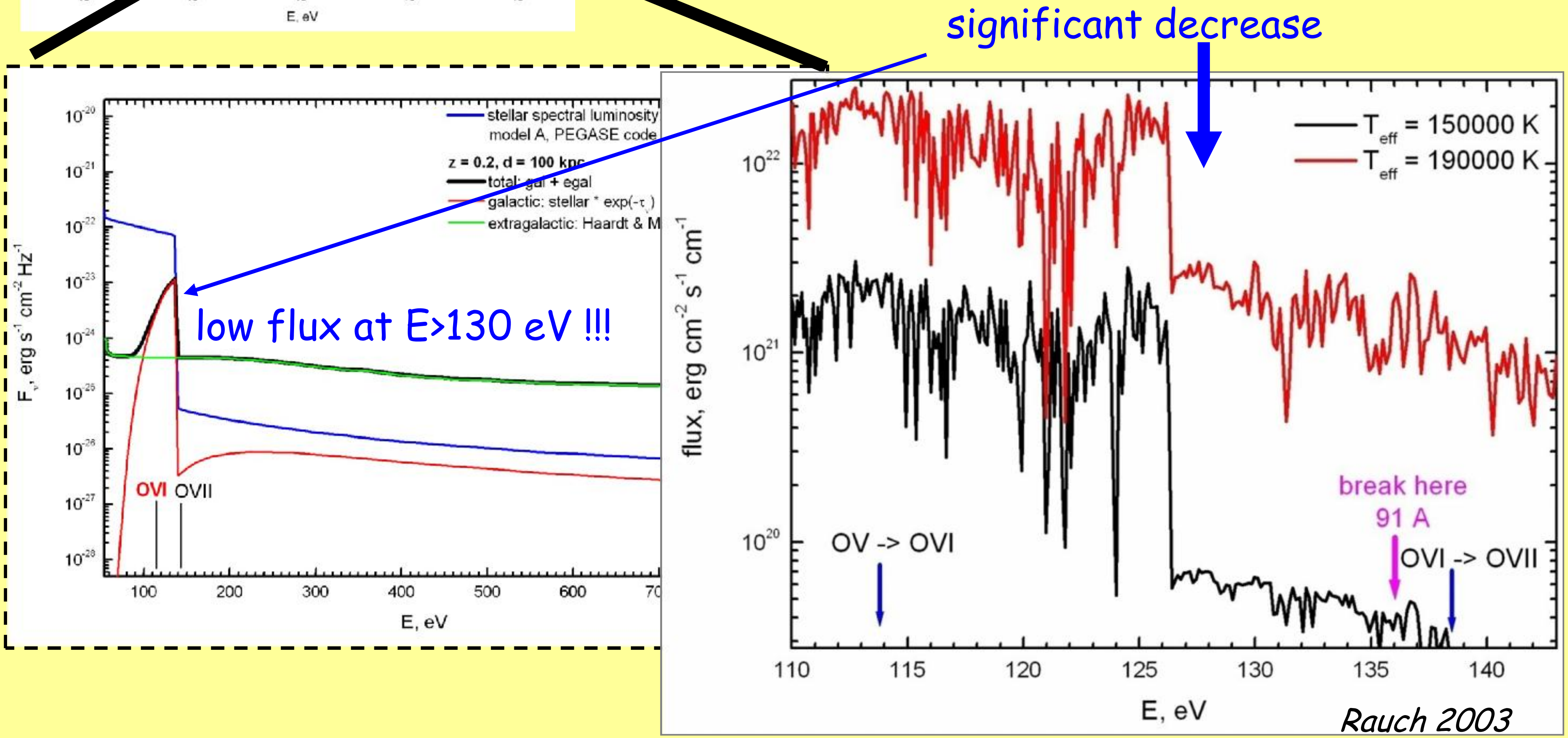

 implications: circumgalactic OVI

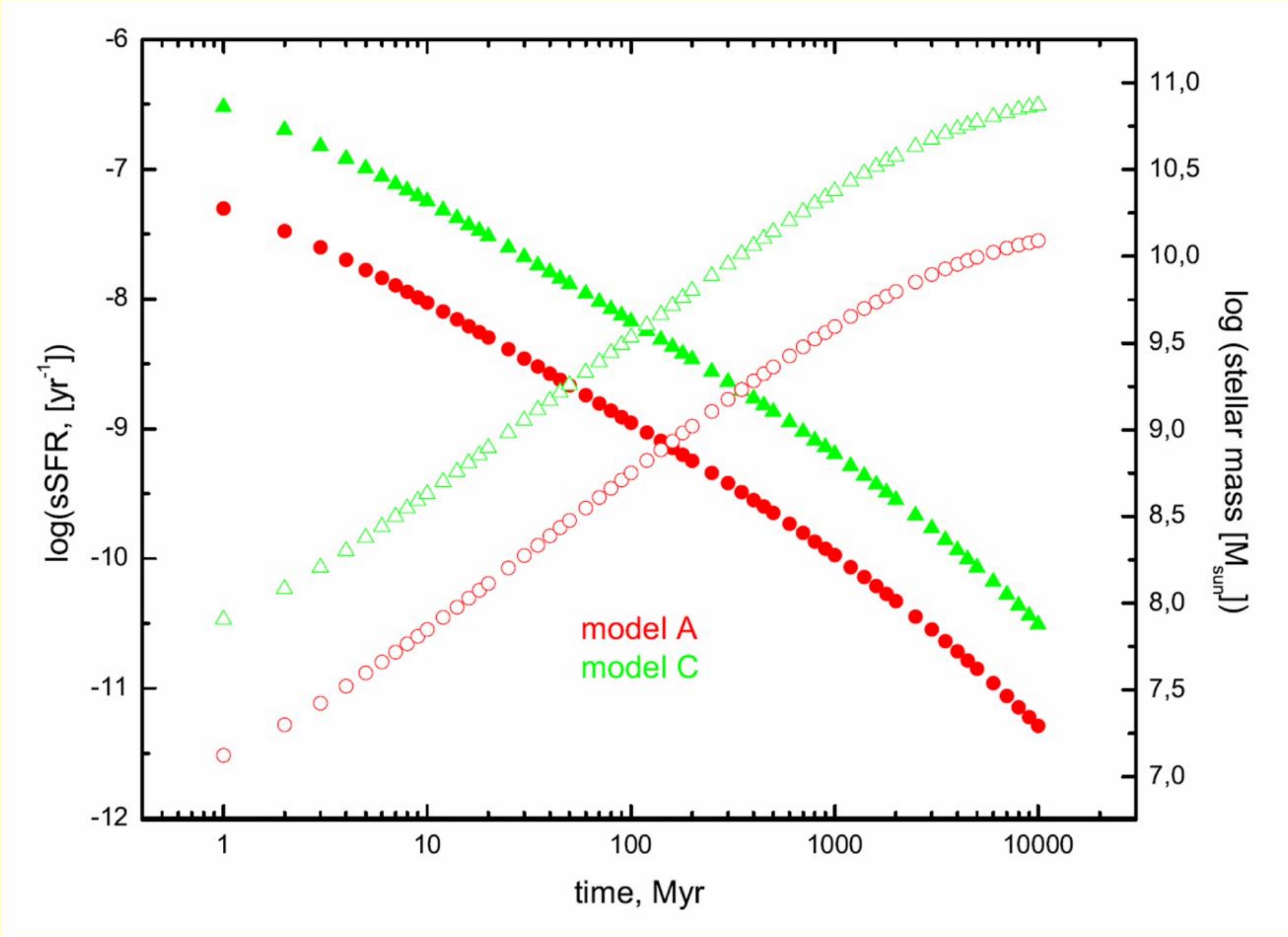

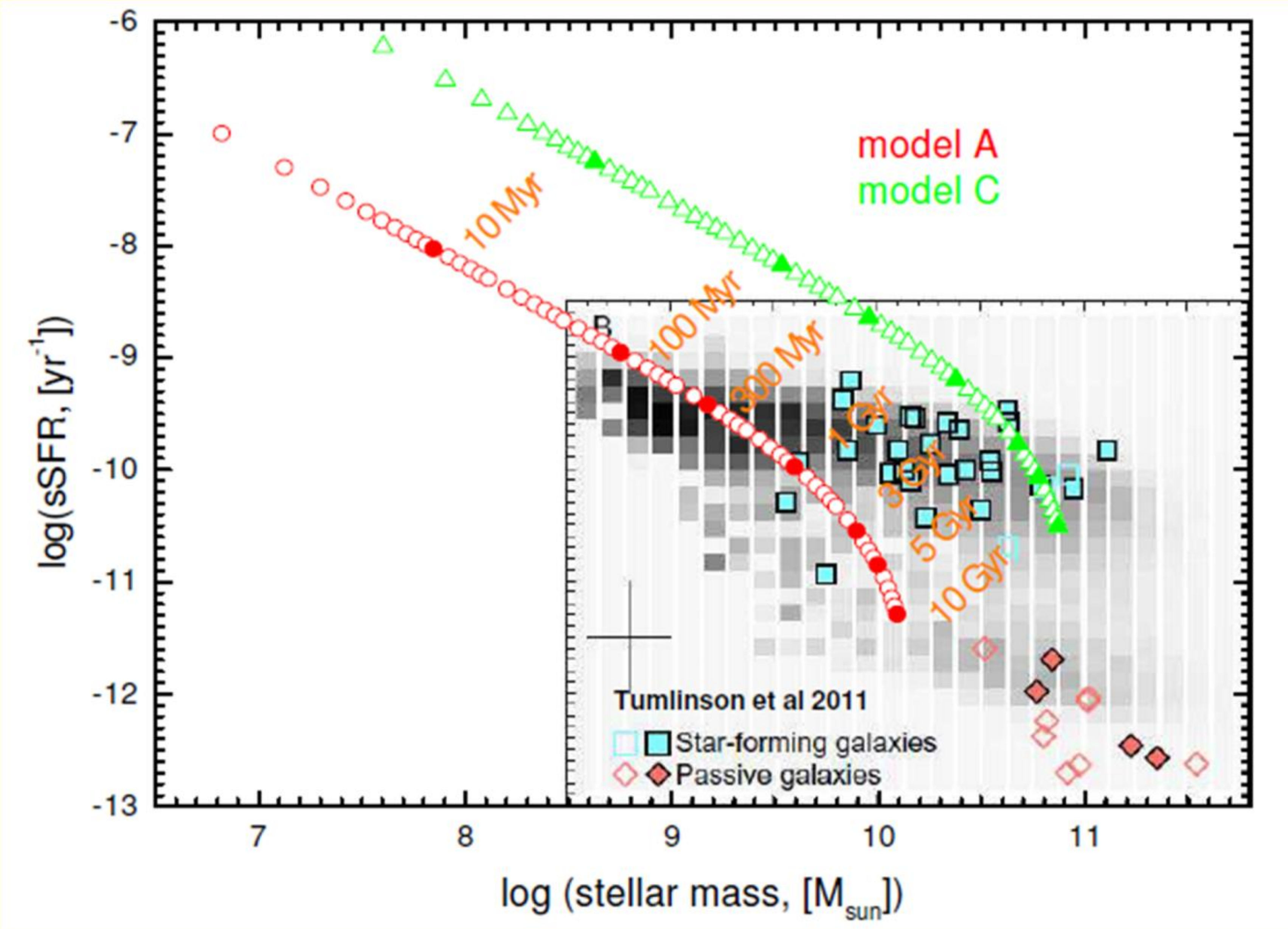
model A
model C
10 Myr
100 Myr
300 Myr
1 Gyr
3 Gyr
5 Gyr
10 Gyr
B
Tumlinson et al 2011
Star-forming galaxies
Passive galaxies
log(sSFR, [yr^{-1}])
log (stellar mass, [M$_{sun}$])
-6
-7
-8
-9
-10
-11
-12
-13
7
8
9
10
11

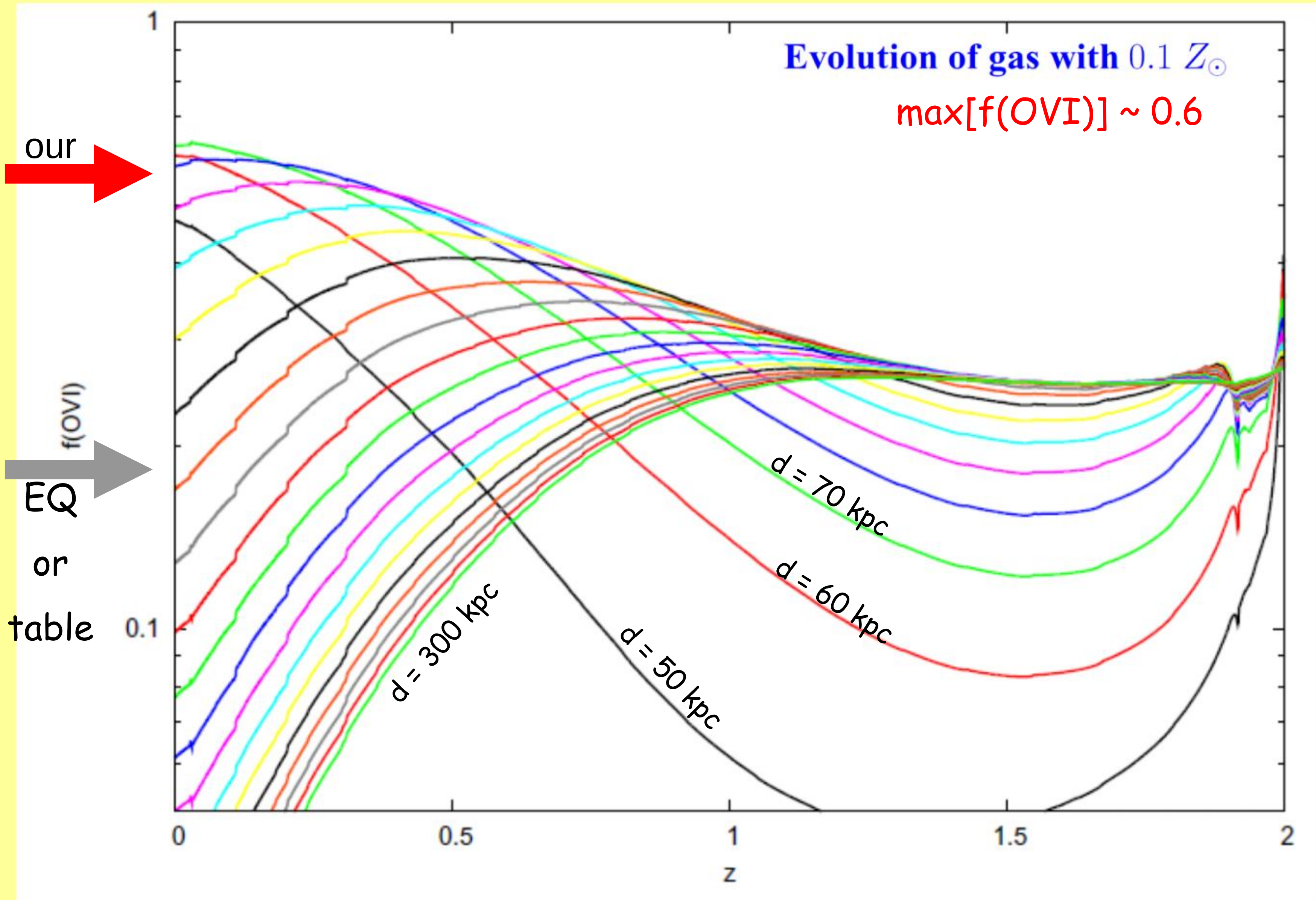

decrease the oxygen mass (at least) in 2-3 times metals in the IGM/CGM/ISM: **implications: circumgalactic OVI**

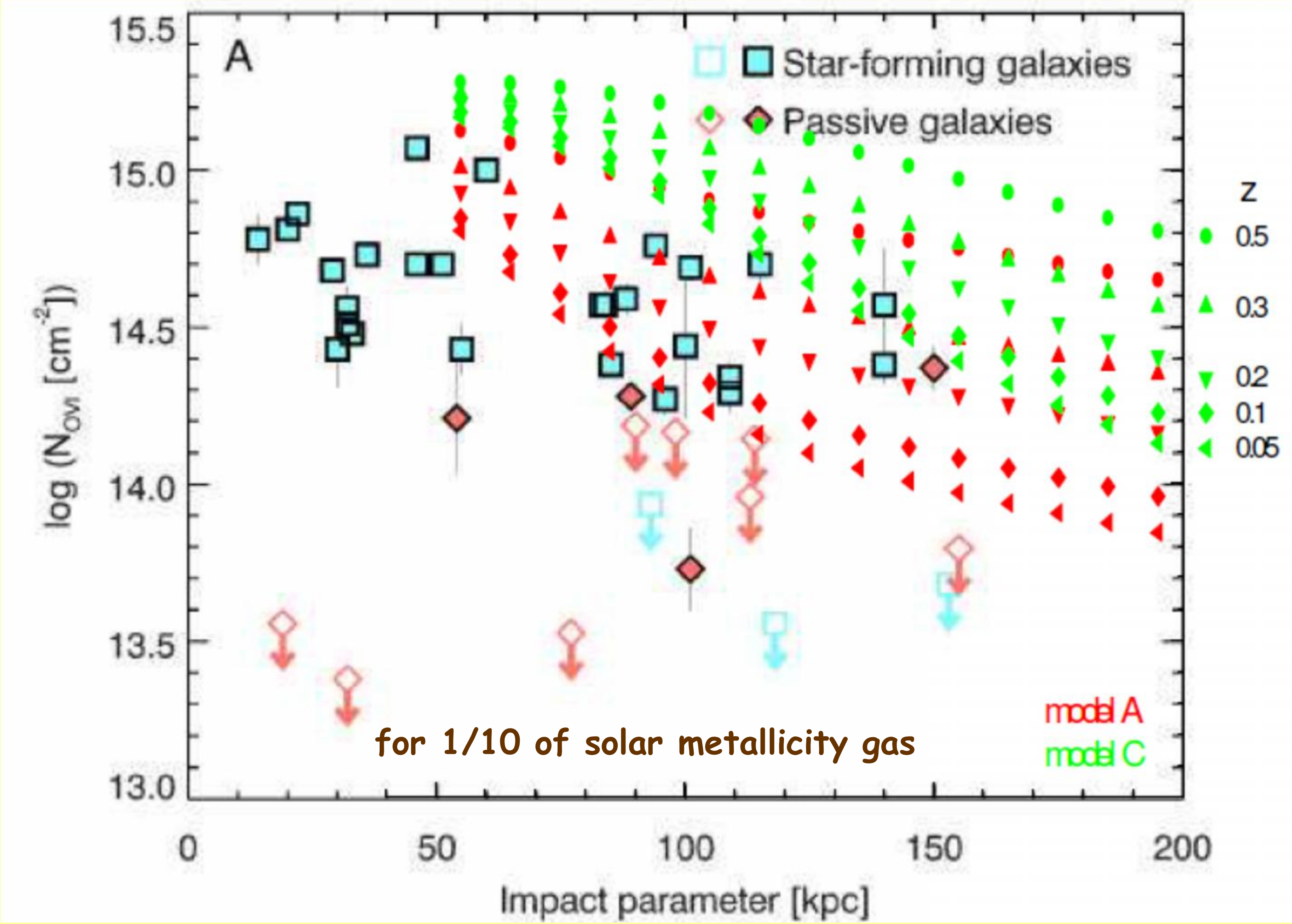

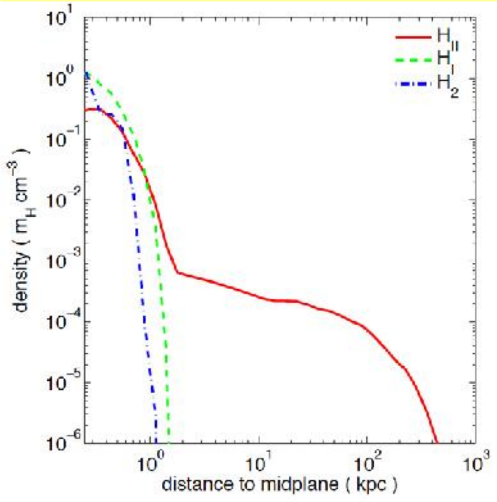

Feldmann etal 2012

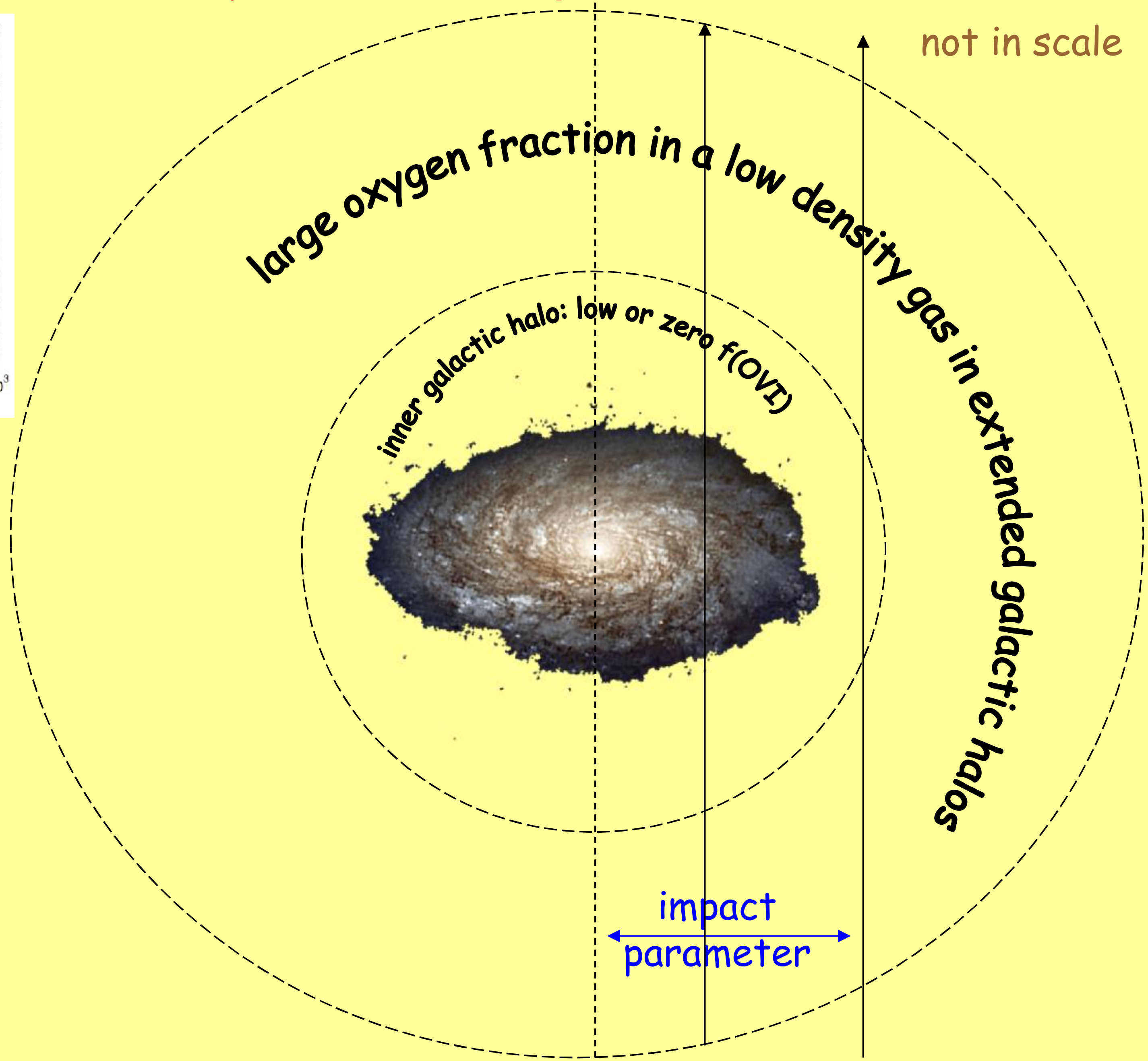

metals in the IGM/CGM/ISM: **implications: circumgalactic OVI**

$$N_{\rm OVI} = L\left(\frac{n_{\rm O}}{n_{\rm H}}\right)\left(\frac{\rho}{m_{\rm H}}\right)\left(\frac{Z}{Z_\odot}\right) = 10^{14} L_{\rm kpc}\left(\frac{\rho/\bar{\rho}}{1000}\right)\left(\frac{f_{\rm OVI}}{0.2}\right)\left(\frac{Z}{Z_\odot}\right)\ {\rm cm}^{-2},$$

$$M_{\rm OVI} = \pi R^2 N_{\rm OVI}(16 m_H).$$

Tumlinson et al 2011

$$M_{\rm O} = 1.2\times10^{7} M_\odot \left(\frac{R}{150\,{\rm kpc}}\right)^2 \left(\frac{N_{\rm OVI}}{10^{14.5}\,{\rm cm}^{-2}}\right)\left(\frac{0.2}{f_{\rm OVI}}\right),$$

decrease the oxygen mass (at least) in 2-3 times

max[f(OVI)] ~ 0.6; f(OVI) [b<130 kpc] > 0.2

for 1/10 of solar metallicity gas

log(OVI) ~14.5 – 15.3 cm^{-2}

for 1/100 of solar metallicity: logN(OVI) ~12.9 – 14.2 cm^{-2}

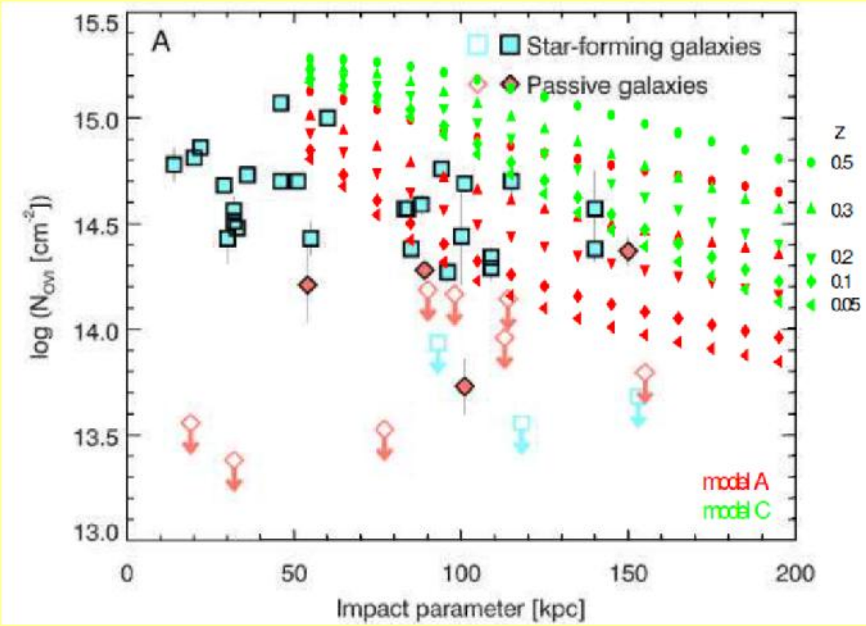

$$N_{\rm OVI} = L\left(\frac{n_{\rm O}}{n_{\rm H}}\right)\left(\frac{\rho}{m_{\rm H}}\right)\left(\frac{Z}{Z_\odot}\right) = 10^{14} L_{\rm kpc}\left(\frac{\rho/\bar{\rho}}{1000}\right)\left(\frac{f_{\rm OVI}}{0.2}\right)\left(\frac{Z}{Z_\odot}\right)\ {\rm cm^{-2}},$$

$$M_{\rm OVI} = \pi R^2 N_{\rm OVI}(16 m_H).$$

Tumlinson et al 2011

$$M_{\rm O} = 1.2\times10^7 M_\odot \left(\frac{R}{150\,{\rm kpc}}\right)^2 \left(\frac{N_{\rm OVI}}{10^{14.5}\,{\rm cm^{-2}}}\right)\left(\frac{0.2}{f_{\rm OVI}}\right),$$

decrease the oxygen mass (at least) in 2-3 times

max[f(OVI)] ~ 0.6; f(OVI) [b<130 kpc] > 0.2

for 1/10 of solar metallicity gas

in NEQ !!!

log(OVI) ~14.5 – 15.3 cm^{-2}

for 1/100 of solar metallicity: log(OVI) ~12.9 – 14.2 cm^{-2}

in EQ !!!

densities it is hard to produce a 10 cm column density within the confines of a galactic halo, especially if the metallicity is low (Fig. S5). Thus $f_{\rm OVI} = 0.02$ and $Z = 0.1 Z_\odot$ are plausible conditions for the O VI-traced gas, but it is unlikely that both conditions hold simultaneously. However, if either one holds the CGM detected here could represent an important contribution to the cosmic budgets of metals and baryons. In either case M is compara-

Tumlinson et al 2011

M_{gas} (r<300 kpc) ~ 3×10^{10} M_{sun} at low z

HI measurements (Prochaska etal 2011)

M_{gas} (in CGM) ~ 4×10^{10} M_{sun}

in SF galaxies at z = 2-3 (Steidel etal 2010)

Z/Zsun	M_{oxygen}
1	~ 2×10^{8} M_{sun}
1/10	~ 2×10^{7} M_{sun}

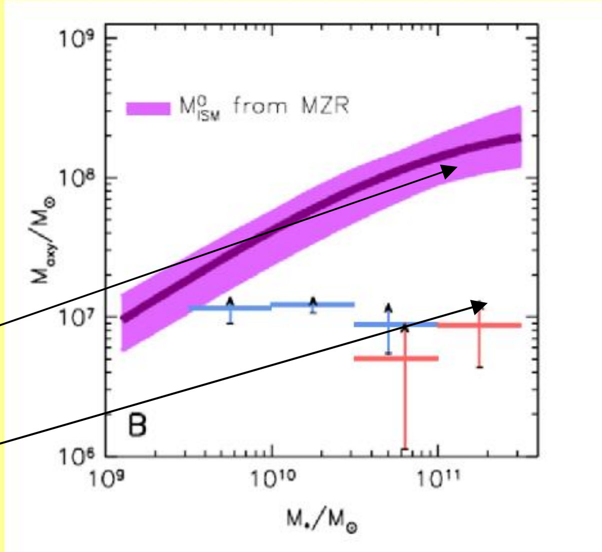

M_{gas} (r<300 kpc) ~ 3×10^{10} M_{sun} at low z

HI measurements (Prochaska etal 2011)

M_{gas} (in CGM) ~ 4×10^{10} M_{sun}

in SF galaxies at z = 2-3 (Steidel etal 2010)

Z/Zsun	M_{oxygen}
1	~ 2×10^{8} M_{sun}
1/10	~ 2×10^{7} M_{sun}

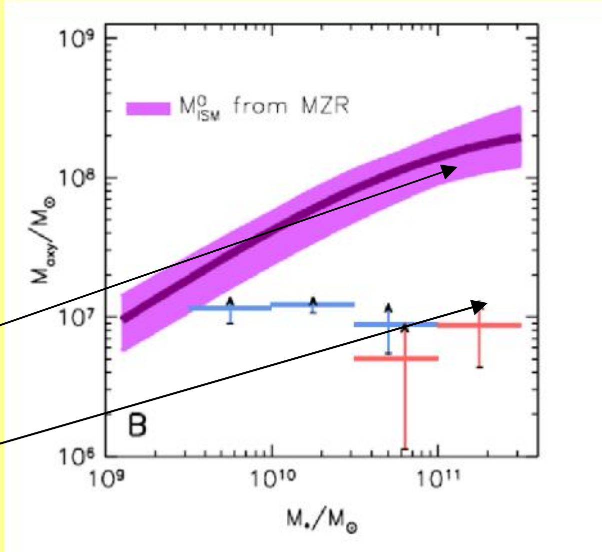

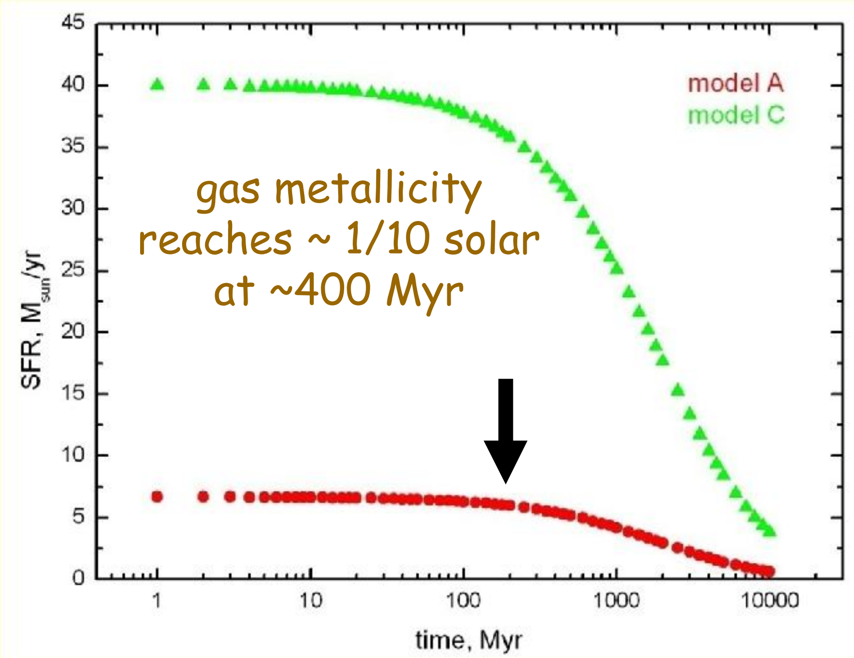

1 solar mass of SFR gives 0.015 solar mass of oxygen

Mass of oxygen ~

6 M_{sun}/yr x 200 Myr x 0.015 ~ **2 x 10^{7} M_{sun}**

outflows:

~100 km/s x 1 Gyr ~ **100 kpc**